Parameter Planes for Complex Analytic Maps *

Robert L. Devaney†
Department of Mathematics
Boston University
111 Cummington Mall
Boston, MA 02215 USA

May 20, 2013

Abstract

In this paper we describe the structure of the parameter planes for certain families of complex analytic functions. These families include the quadratic polynomials $z^2 + c$, the exponentials $\lambda \exp(z)$, and the family of rational maps $z^n + \lambda/z^n$. These are, in a sense, the simplest polynomial, transcendental, and rational families, as each has essentially one critical orbit.

*2000 MSC number: Primary 37F10; Secondary 37F45
†This work was partially supported by grant #208780 from the Simons Foundation.

In this paper we give a brief overview of the structure of the parameter plane for three different families of complex analytic maps, namely quadratic polynomials (the Mandelbrot set), singularly perturbed rational maps, and the exponential family. The goal is to show how these objects allow us to understand almost completely the different dynamical behaviors that arise in these families as well as the accompanying bifurcations.

1 The Mandelbrot Set

The Mandelbrot set $\mathcal{M}$ is one of the most interesting and beautiful objects in all of mathematics. Amazingly, it arises as the parameter plane for the seemingly simple quadratic family $P_c(z) = z^2 + c$. See Figure 1. This is a picture in the c-plane (the parameter plane) that describes the fate of the orbit of the only critical point for this family, namely 0. If the orbit of 0 does not tend to ∞, then the corresponding parameter c lies in $\mathcal{M}$ and we color this point black. If the orbit does escape to ∞, then c is not in the Mandelbrot set and we color c according to how quickly the orbit of 0 reaches the exterior of a large disk surrounding the origin (with red points escaping fastest, followed in order by orange, yellow, green, blue, and violet.

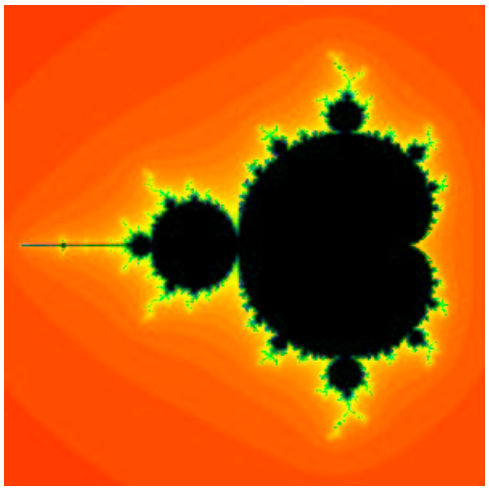

Figure 1: The Mandelbrot set. Colored points are c-values for which the orbits of 0 escape to ∞; black points are c-values for which this does not happen. So the Mandelbrot set is the black region in these images.

In complex dynamics, the object of central interest in the dynamical plane is the *Julia set*. For the family P_c, there is an open neighborhood of ∞ in the Riemann sphere consisting of points whose orbits tend to ∞. The set of all points whose orbits tend to ∞ is called the basin of ∞. Then the Julia set, denoted by $J(P_c)$ is the boundary of this basin. There are other equivalent definitions of $J(P_c)$. For example, it is known that $J(P_c)$ is also the closure of the set of repelling perioidc points of P_c. As a consequence, we see that the Julia set is the chaotic set, for arbitrarily close to any point in $J(P_c)$, we have points whose orbits are periodic and other points whose orbits tend to ∞. In fact, via Montel's Theorem, given any point in the Julia set, then any open neighborhood of this point, no matter how small, is eventually mapped over the entire complex plane, minus at most one point. So the family of iterates of P_c on the Julia set is very sensitive to initial conditions. The *filled Julia set* is, by definition, the set of all points whose orbits do not tend to ∞. So $J(P_c)$ is also the boundary of the filled Julia set. The *Fatou set* is then the complement of $J(P_c)$ in the Riemann sphere.

The natural question is: Why are we interested in the fate of the orbit of the critical point? Well, in short, the critical orbit "knows it all" in complex dynamics. In particular, for the family P_c, if the orbit of 0 tends to ∞, then the Julia set of P_c is a Cantor set. If the orbit of 0 does not escape to ∞, then $J(P_c)$ is a connected set. So there are only two possible types of Julia sets for P_c: those that consist of uncountably many point components, and those that consist of exactly one component. There are no Julia sets for quadratic polynomials that consist of 2 or 20 or 200 components.

The large black open regions visible in the Mandelbrot set are regions for which P_c has an attracting cycle of some given period. It is known that, if P_c has an attracting cycle, then the orbit of the critical point must tend to this cycle. Hence there can be at most one attracting cycle for a quadratic polynomial. For example, any c-value drawn from the central cardioid has an attracting fixed point. For c in the large open disk just to the left of this cardioid, P_c has an attracting 2-cycle. We thereforecall this the period 2-bulb. And, for c in the northernmost and southernmost bulbs off the main cardioid, P_c has an attracting cycle of period 3, so these are the period 3-bulbs. Such open disks are called *hyperbolic components*, since it is known that P_c must then be hyperbolic on the Julia set, i.e., in some suitable metric, P_c is everywhere expanding.

As c moves from one hyperbolic component to another, the map undergoes a bifurcation. The simplest part of this bifurcation is the fact that we

move from having an attracting cycle of some period when we are in one hyperbolic component to having an attracting cycle of some other period in the subsequent hyperbolic component. But, if fact, much more happens: the topology of the Julia sets changes dramatically. For example, if we move from the main cardioid to the period-2 bulb, the Julia set, which is just a simple closed curve when c is in the main cardioid, becomes a "basilica" when c is in the period 2-bulb. What happens is a repelling 2-cycle that lies in $J(P_c)$ when c is in the cardioid suddenly merges with the attracting fixed point and thereby makes it neutral when the parameter reaches the boundary of the cardioid. So two points in $J(P_c)$ become identified to one point. Meanwhile, infinitely many pairs of preimages of this point also become identified. This is what accounts for the infinitely many "pinch-points" visible in the basilica. Or, as we move from the main cardioid to the period 3-bulbs, a period 3-cycle becomes identified and the Julia set transforms into the "Douady rabbit." See Figure 2. You may construct an animation to view these bifurcations by using the Mandelbrot Movie Maker applet at the website `http://math.bu.edu/DYSYS/applets`.

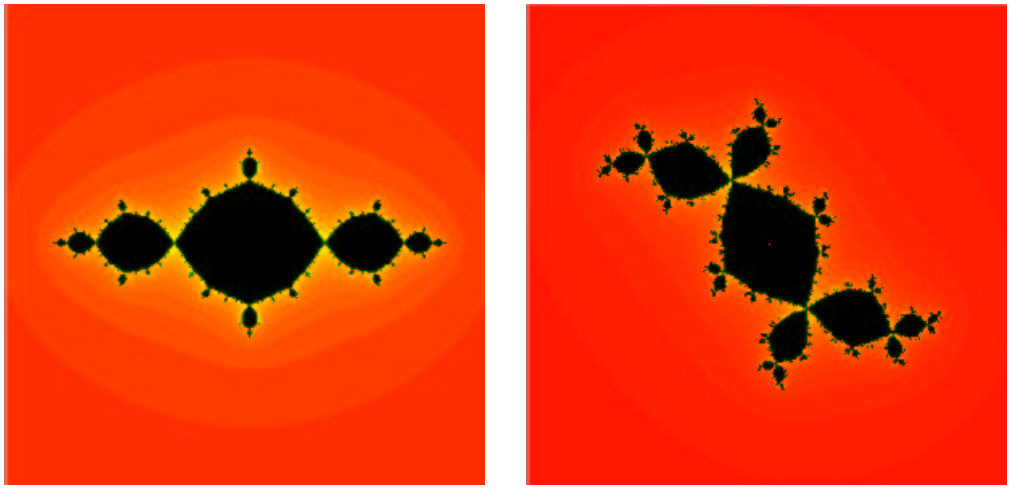

Figure 2: The Julia sets for $z^2 - 1$ (the basilica) and $z^2 - 0.12 + .75i$ (the Douady rabbit). The filled Julia sets are the black regions, so the Julia sets here are the boundaries between the black and colored regions.

Along the boundaries of these hyperbolic components is where things get

complicated. At each c-value on the boundary, P_c has a neutral cycle, i.e., a periodic point z of period n for which $(P_c^n)'(z) = \exp(2\pi i\theta)$. As c winds once around the boundary of this hyperbolic component, θ winds once around the unit circle. As a consequence, there is a dense set of such c's for which θ is rational. In this case, the neutral cycle lies in the Julia set but there are still regions in which all points tend to the neutral cycle (although these regions no longer surround the points on the cycle). These types of periodic points are called *parabolic points*.

The case where θ is irrational is much more complicated. If θ is highly irrational (i.e., "far" from rationals), then there is an open disk around each point on the cycle on which P_c^n is conjugate to the irrational linear rotation of angle θ. These disks are called Siegel disks. When θ is close to rationals, the structure of the Julia set near this cycle is still not completely understood. This is one of the major open problems in complex dynamics. See [16] for details.

A natural question is how do we understand how all of the bulbs and other smaller Mandelbrot sets are arranged in $\mathcal{M}$. Amazingly, if we zoom in to any portion of the boundary of the Mandelbrot set, it turns out that this zoom is very different from any other zoom that is non-symmetric with respect to $c \mapsto \overline{c}$. More importantly, with a keen eye for geometry, one can deduce exactly where in the boundary of $\mathcal{M}$ this zoom is, and, more importantly, what the corresponding dynamical behavior in the associated bulb is. It turns out that there are several different geometric and dynamical ways to understand the structure of these bulbs. First we will look at this geometrically, and then, using complex analysis, we will indicate how to prove this.

For simplicity, let's concentrate on the bulbs attached to the main cardioid. How do we know what their period is? One way is easy: look at the bulb. There is an antenna attached to this bulb. This antenna has a junction point from which a certain number of spokes emanate. The number of these spokes tells us exactly what the period is. For example, in Figure 3, we display two bulbs having periods 5 and 7. Note that this is the exact number of antennas hanging off the junction point in the antenna of each bulb.

There is another way to read off the periods of these bulbs. Choose a parameter from the interior of a period n bulb and plot the corresponding filled Julia set. There is a central disk in these filled Julia sets that surrounds the origin. Then there are exactly $n-1$ smaller disks that join this main disk at certain junction points. For example, in Figure 2, we see that the

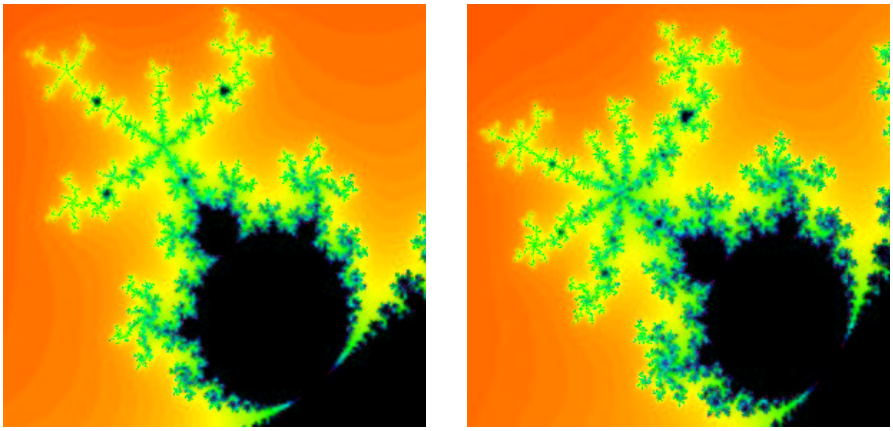

Figure 3: Period 5 and 7 bulbs hanging off the main cardioid.

rabbit has two "ears" attached to the central disk and the period of this bulb is $2 + 1 = 3$. Similarly, the basilica has just 1 ear and the period here is $1 + 1 = 2$. In Figure 4, we display Julia sets from the above period 5 and period 7 bulbs, and we see the same phenomenon. The Mandelbrot/Julia Set applet at the website `http://math.bu.edu/DYSYS/applets` allows you to view and zoom in on the Mandelbrot and Julia sets of P_c to see more examplese of these phenomena.

Now let us turn to the arrangement of the bulbs around the main cardioid. Recall that, on the boundary of the main cardioid, P_c has a fixed point whose derivative is given by $\exp(2\pi i\theta)$. Then a little algebra shows that a parametrization of the boundary of this main cardioid is given by

$$c = c(\theta) = \frac{e^{2\pi i\theta}}{2} - \frac{e^{4\pi i\theta}}{4}.$$

So when $\theta = 0$, $c = 1/4$ and we are at the cusp of the main cardioid; when $\theta = 1/2$, $c = -3/4$, and we are at the point where the period 2-bulb meets the main cardioid. In general, when θ is a rational number p/q in lowest terms, the corresponding c-value lies at the meeting point (also called the root point) of the main cardioid and a period q-bulb which we now call the p/q-bulb. So we see that the bulbs are arranged around the main cardioid in the exact order of the rational numbers. In particular, we can count exactly how many period q-bulbs there are. For example, there are 6 period 7-bulbs and 4 period 10-bulbs touching the main cardioid.

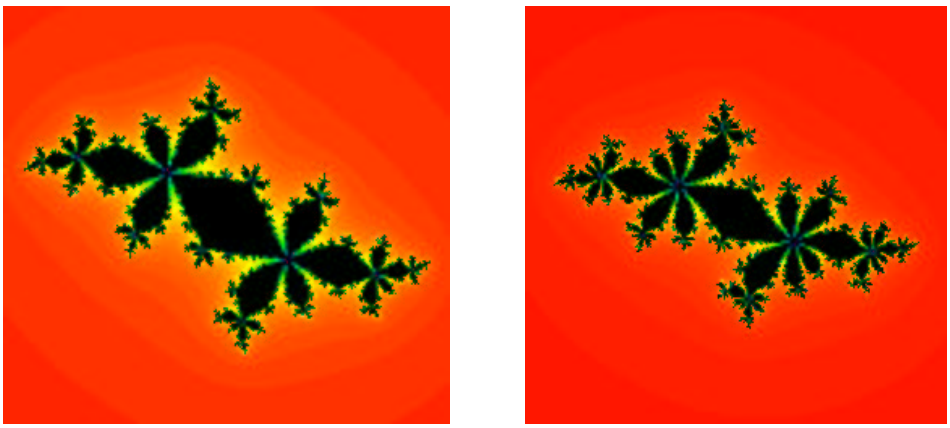

Figure 4: Julia sets drawn from the above period 5 and 7 bulbs hanging off the main cardioid. Note that there are 4 and 6 "ears" hanging off the central disks of these filled Julia sets.

But there are several other geometric and dynamical ways to understand this. Look at the period five bulb in Figure 3. We call the spoke of the antenna that extends down to the bulb from the junction point the *principal spoke*. Note that the "shortest" spoke (that is not the principal spoke) is located 2/5 of a turn in the counter-clockwise direction from the principal spoke. And this bulb is exactly the 2/5-bulb. In that same figure, we also see that the period 7-bulb is, in fact, the 3/7-bulb.

A second way to see this is to turn to the filled Julia set. In Figure 4, each of the filled Julia sets has a main component that surrounds the origin together with $q-1$ ears attached at one point. Note where the "smallest" ear is located; it is exactly p/q of a turn in the counterclockwise direction from main component.

And then there is a third way to read off p/q. Simply plot the points on the attracting cycle of period q in the Fatou set. What you see is that this cycle moves around the ears and the main component, rotating by p/q of a turn at each stage. So there is a very nice connection between the geometry of the Mandelbrot set and Julia sets and the dynamics of P_c.

One natural question that arises is: What is meant by the "shortest" spoke or the "smallest" ear? To make these ideas precise, we turn to the

Riemann Mapping Theorem.

First recall that we have a basin of ∞ that is an open disk in the Riemann sphere whenever c is chosen to lie in $\mathcal{M}$. Call this basin B_c. Then it is known that we can construct and analytic homeomorphism ϕ_c that takes B_c to the open unit disk $\mathbb{D}$ and maps ∞ to 0. Moreover, ϕ_c conjugates P_c on B_c with the simple map $z \mapsto z^2$ on $\mathbb{D}$. That is,

$$\phi_c(P_c(z)) = (\phi_c(z))^2.$$

In particular, the map z^2 takes the straight ray of angle θ given by $te^{i\theta}$ for $0 < t < 1$ to the ray $te^{i2\theta}$, the ray of angle 2θ. Then the preimage under ϕ_c^{-1} of the straight ray of angle θ in B_c is called the external ray of angle θ, and P_c interchanges these external rays just as $z \mapsto z^2$ interchanges the straight rays.

Now it is a fact that, when P_c has an attracting cycle, each of these external rays lands at a unique point in $J(P_c)$. The reason for this is that P_c is hyperbolic on $J(P_c)$ and consequently the Julia set is locally connected. When c is chosen from the main cardioid, each external ray has a unique landing point, so this says that P_c is conjugate to $z \mapsto z^2$ on its Julia set. But, when c lies in other bulbs, certain of these rays land at the same point. It is true that the external ray of angle 0 always lands at a particular fixed point in $J(P_c)$ and this is the only such ray landing at this point. Similarly, the external ray of angle $1/2$ is the unique ray landing at the preimage of this fixed point. But, when c is chosen from the p/q-bulb, there is a fixed point that lies on the boundary of the main Fatou component containing 0 and is the connection point for the q basins of the attracting cycle. Now there are exactly q rays that land at this fixed point. Moreover, P_c must interchange these rays just as above, by angle-doubling.

So, for example, when c is in the $2/5$-bulb, there must be five rays of angle $\theta_0, \ldots, \theta_4$ that land on this fixed point. And they must be mapped around just as P_c interchanges the ears in the Julia set, so

$$\theta_0 \mapsto \theta_1 \mapsto \theta_2 \mapsto \theta_3 \mapsto \theta_4 \mapsto \theta_0 \ldots.$$

Then a little computation shows that $\theta_0 = 9/31$, so that $\theta_1 = 18/31$, $\theta_2 = 5/31$, $\theta_3 = 10/31$, and $\theta_4 = 20/31$. In similar fashion, the external rays that land at the fixed point on the main component of a Julia set when c is in other p/q-bulbs may also be calculated.

So, how do we determine the size of the "ears" on these Julia sets? Using what is called *harmonic measure*, we define the size of the ears just to be the

difference of the angles of the two landing external rays that separate this ear from the other components containing the attracting cycle. So, in the 2/5 case, we see that the smallest ear is contained between the external rays of angles $\theta_0 = 9/31$ and $\theta_3 = 10/31$, so this ear has "size" $10/31 - 9/31 = 1/31$, whereas all the other ears are larger.

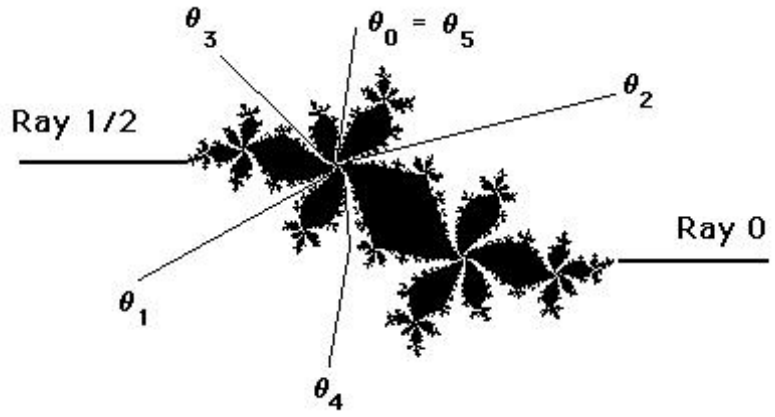

Figure 5: The orbit $\theta_0 \to \theta_1 \to \theta_2 \ldots$ of the rays landing at the fixed point $J(P_c)$ when c is in the 2/5 bulb.

Now how do we determine the size of the spokes of the antennas in the Mandelbrot set? We use essentially the same technique, but now in the parameter plane. Using a celebrated result of Douady and Hubbard [11], there is a similar "uniformization" of the exterior of $\mathcal{M}$ in the Riemann sphere which again maps ∞ to 0. Let $\mathcal{C}$ denote this external region. To construct this map, for each $c \in \mathcal{C}$, we have that the critical value c for P_c now lies in B_c. So we can consider the function $\Phi(c) = \phi_c(c)$. Just as in the previous case, Φ is now an analytic homeomorphism that takes $\mathcal{C}$ onto $\mathbb{D}$. So again we have external rays, but now they are in the parameter plane. It is known that all rational rays land at a unique point on the boundary of the Mandelbrot set. Some land at root points of bulbs or cusp points on the cardioids of small copies of the Mandelbrot set. Others land at the endpoints of the spokes of the antennas or at the junction points. And one can use similar tehniques as above to determine exactly where certain of these external rays land. See [5], [8]. For example, it is known that, if an external ray of angle θ lands at the root point of a period q-bulb, then the angle

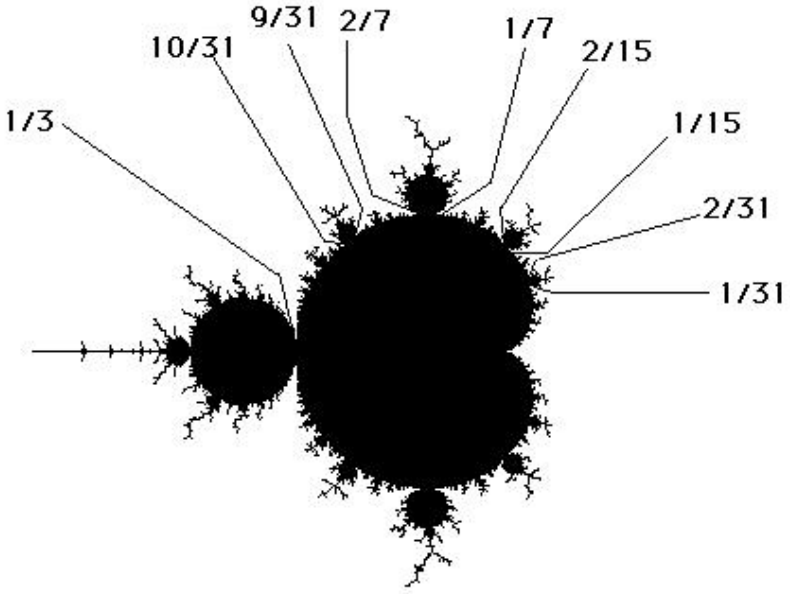

Figure 6: Rays landing on the Mandelbrot set.

θ must have period q under angle-doubling. So, for example, the two rays landing at the root point of the period 2-bulb must be $1/3$ and $2/3$. The rays landing at the northern period 3-bulb are $1/7$ and $2/7$ and at the southern period 3-bulb are $5/7$ and $6/7$. So the rays $3/7$ and $4/7$ must also land on a period 3-bulb that is somewhere to the left of the northern and southern period 3-bulbs. Indeed, as is well-known, there is a small Mandelbrot set lying along the negative real axis whose main cardioid contains parameters for which there is an attracting 3-cycle. So these two external rays both land at the cusp of this main cardioid.

One curious fact that relates to the Farey tree involves the size of the bulbs hanging off the main cardioid. To begin, we think of the root point of the main cardioid as being the cusp at $c = 1/4$. Then we call the main cardioid the $0/1$-bulb. Which is the largest bulb between the root points of the $0/1$ and $1/2$-bulbs (in, say, the upper portion of $\mathcal{M}$)? It is clearly the $1/3$-bulb. And note that $1/3$ is obtained from the previous two fractions by *Farey addition*, i.e., adding the numerators and adding the denominators

$$\frac{0}{1} \text{“}+\text{”} \frac{1}{2} = \frac{1}{3}.$$

Similarly, the largest bulb between the 1/3 and 1/2-bulbs is the 2/5-bulb, again given by Farey addition. As above, we again measure the size of these bulbs by determining the interval of external rays that land on the bulb. So the size of the period 3-bulb is $2/7 - 1/7 = 1/7$ while the 2/5-bulb has size 1/31, as seen in Figure 6. Note that the 2/5-bulb is the largest bulb between the 1/2 and 1/3-bulbs. Then this process continues. The largest bulb between the 2/5 and 1/2-bulb is the 3/7-bulb and the largest bulb between the 2/5 and 1/3-bulbs is the 3/8-bulb and so on along the "Farey tree."

One of the most interesting and important open problems in complex dynamics is the question of whether or not the boundary of the Mandelbrot set is locally connected. If this is the case, then all of the external rays land at unique points along the boundary of $\mathcal{M}$. As a consequence, we would understand everything about the Mandelbrot set. However, it is not at all clear that this boundary is locally connected. Think about the period one-millionth bulb — the antenna here has a million spokes! And as the denominators of p/q get larger, the antenna structure also becomes even more "complex." It is true that the size of these bulbs gets smaller as q increases, so it is possible that the boundary is locally connected. However, a result of Shishikura [19] shows that the boundary of $\mathcal{M}$ has Hausdorff dimension 2, so, indeed, this boundary is pretty "crazy." Furthermore, a result of Buff and Chéritat [1] shows that Julia sets of P_c that contain fixed points that are close to rationals have positive Lebesgue measure, something that also indicates that things are getting quite complicated along the boundary of $\mathcal{M}$.

2 Singularly Perturbed Rational Maps

We now consider a very different type of map, namely rational maps of the form

$$F_\lambda(z) = z^n + \frac{\lambda}{z^n}$$

where $n \geq 2$. While the degree of these maps can be quite large, there is really only one "free" critical orbit just as in the case of quadratic polynomials. Indeed, one checks easily that there are $2n$ critical points given by $\lambda^{1/2n}$. However, there are only two critical values $\pm 2\sqrt{\lambda}$; n of the critical points map to one critical value and the other critical points map to the second

critical value. But, when n is even, both critical values then map to the same point, whereas, if n is odd, we have $F_\lambda(-z) = -F_\lambda(z)$, so the two critical values have orbits that are symmetric under $z \mapsto -z$. We call this the free critical orbit, since ∞ and 0 are also critical points, but ∞ is fixed and 0 is mapped by F_λ onto ∞.

Just as in the case of $z^2 + c$, the point at ∞ is an attracting fixed point when $n \geq 2$, so we have an immediate basin of attraction B_λ of ∞ that lies in the Fatou set. Also, 0 is a pole, so there is a neighborhood of 0 that is mapped into B_λ. If the component of the Fatou set containing 0 is disjoint from B_λ, we denote this set by T_λ and call it the trap door since any orbit that eventually ends up in B_λ must pass through T_λ. This follows since F_λ maps both B_λ and T_λ n-to-1 onto B_λ and the map F_λ has degree $2n$.

Unlike the quadratic polynomial case, where we had only one possibility for the structure of the Julia set when the critical orbit escapes, here we have an escape trichotomy. As shown in [9],

1. If the critical values lie in B_λ, then $J(F_\lambda)$ is a Cantor set;

2. If the critical values lie in T_λ, then $J(F_\lambda)$ is a Cantor set of simple closed curves;

3. In all other cases, the Julia set is connected. If the critical orbit enters B_λ at iteration 2 or later, then $J(F_\lambda)$ is a Sierpinski curve.

The second result here is due to McMullen [15]. Incidentally, case 2 does not occur when $n = 2$; indeed the situation when $n = 2$ is very different from (and much more complicated than) the case $n > 2$ [6].

A Sierpinski curve is any planar set that is homeomorphic to the well-known Sierpinski carpet fractal displayed in Figure 7. These sets are important for three reasons. First, by a result due to Whyburn [20], there is a topological characterization of any such set: any planar set that is compact, connected, nowhere dense, locally connected, and has the property that any pair of complementary domains are bounded by simple closed curves that are pairwise disjoint is necessarily homeomorphic to the carpet. Second, as proved by Sierpini, the carpet is a universal plane continuum: any planar, one-dimensional, compact curve can be homeomorphically manipulated to fit inside the carpet. And finally, Sierpinski curves occur all the time as Julia sets for rational maps.

In Figure 8, we display the parameter planes (the λ-planes) for the cases where $n = 3$ and $n = 4$. In both cases, the external region is where the

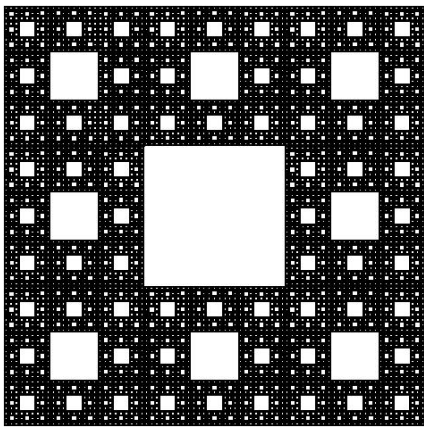

Figure 7: The Sierpinski carpet.

Julia sets are Cantor sets; this is the Cantor set locus. The central disk surrounding the origin contains parameters whose Julia sets are Cantor sets of simple closed curves; we call this region the McMullen domain. All of the other red regions contain parameters whose Julia sets are Sierpinski curves; these are Sierpinski holes.

The arrangement of the Sierpinski holes in the parameter plane is fairly well understood. It is known that there are exactly $(n-1)(2n)^{\kappa-3}$ Sierpinski holes with escape time κ (the number of iterates it takes for the critical orbits to enter B_λ). Each Sierpinski hole contains parameters for which the corresponding maps all have conjugate dynamics on their Julia sets. However, most of the maps drawn from different Sierpinski holes have very diferent dynamics. In fact, only parameters drawn from Sierpinski holes that are symmetric under either complex conjugation or rotation by an $(n-1)^{\text{st}}$ root of unity have conjugate dynamics. Then it follows that, when n is odd, there are exactly $(2n)^{\kappa-3}$ conjugacy classes of maps drawn from Sierpinski holes. When n is even, there are $(2n)^{\kappa-3}/2-2^{\kappa-4}$ such holes. The discrepancy between n odd and even arises because there are no Sierpinski holes along the negative axis when n is odd, whereas there are such holes when n is even. So, when n is odd, there are exactly $2(n-1)$ Sierpinski holes in each conjugacy class, but when n is even, certain conjugacy classes have only $n-1$ Sierpinksi holes. See [10]. In Figure 9, we display four different Sierpinski curve Julia sets drawn from the family when $n = 2$. All of these Julia sets

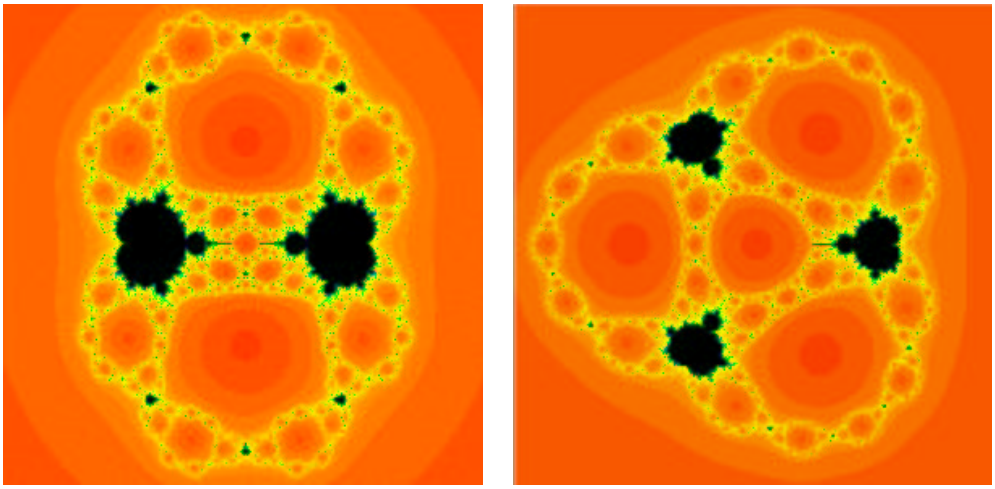

Figure 8: The parameter planes when $n = 3$ and $n = 4$.

are homeomorphic, but it turns out that all have very different dynamics.

One way that Sierpinski curve Julia sets have non-conjugate dynamics occurs when the escape times are different. If F_λ is a map with a Sierpinski curve Julia set for which the critical orbits escape to ∞, then the Fatou components that contain the critical points are the only ones that have boundaries that are mapped 2 to 1 onto their images. So if F_μ has a different escape time, then F_λ cannot be conjugate to F_μ since the boundaries of the escape components containing the critical points would have to be mapped to each other. For escape time Julia sets with the same escape times, many still have non-conjugate dynamics. Proving this involves using Thurston's Theorem [10]. Moreno Rocha [17] has recently produced a dynamical invariant that explains why two such maps have non-conjugate dynamics.

As mentioned earlier, the case $n = 2$ is very different from the case $n > 2$. One reason for this is apparent in Figure 9. Note that, as $\lambda \to 0$, the Julia sets of F_λ seem to converge to the unit disk. Of course, when $\lambda = 0$, we have the very simple map $F_0(z) = z^2$ for which the Julia set is just the unit circle. By Montel's Theorem, if the Julia set ever contains an open set in the plane, then it must be the entire plane. So here we see Julia sets getting closer and closer to the unit disk as $\lambda \to 0$, but, when $\lambda = 0$, things change dramatically. This is why these maps are called singular perturbations.

It is known that there are infinitely many small copies of the Mandelbrot

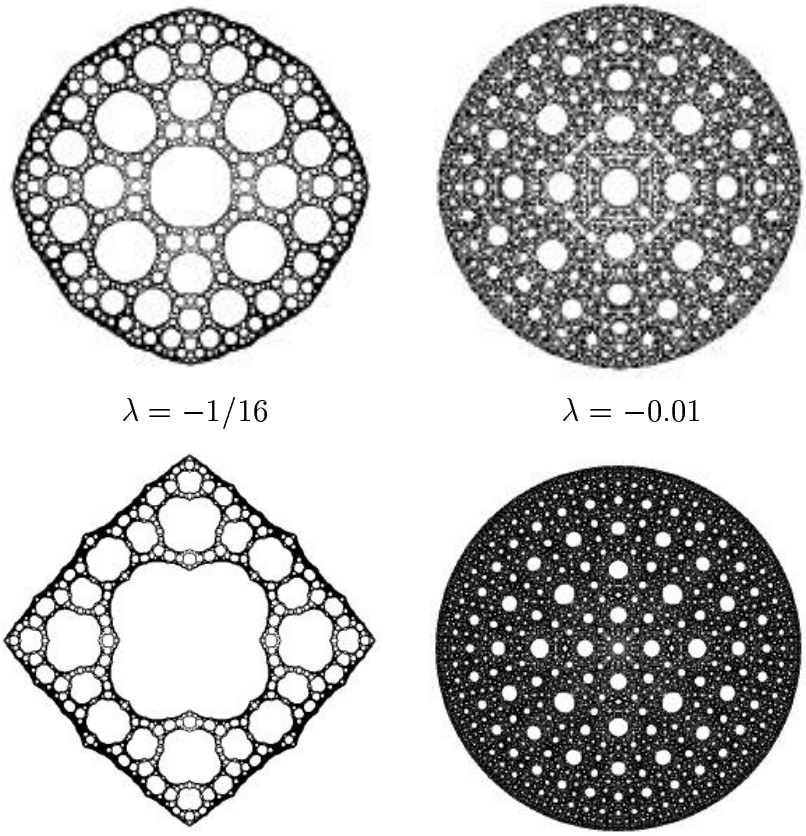

$\lambda = -1/16$ $\lambda = -0.01$

$\lambda = -1/4$ $\lambda = -0.001$

Figure 9: The Julia sets for various values of λ when $n = d = 2$.

set in each of these parameter planes. Certain of the Mandelbrot sets extend out to the boundary of the Cantor set locus while others do not. In these "buried" Mandelbrot sets, Julia sets drawn from the main cardioids are also Sierpinski curves. Since these Julia sets have an attracting cycle of some given period, the dynamics on these Sierpinski curves is quite different than on the escaping Sierpinski curves described above. For parameters in the main cardioids of the Mandelbrot sets that touch the boundary of the Cantor set locus, the structure of the Julia sets is quite different. See [2] for details.

Unlike the Mandelbrot set, these parameter planes have much simpler boundaries. Indeed the boundaries of the Cantor set locus, the McMullen domain, and all of the Sierpinski holes are known to be simple closed curves [18] (when $n > 2$). Of course, as mentioned above, there are also infinitely many small copies of the Mandelbrot set included in these sets, so the full structure in the parameter plane is still at least as complicated as the Mandelbrot set.

3 Complex Exponential Maps

In this final section, we consider another, very different, family of maps, the complex exponential family, $E_\lambda(z) = \lambda \exp(z)$. These are entire transcendental maps, so ∞ is no longer an attracting fixed point. Rather, ∞ is an essential singularity. For the exponential maps there is no longer a critical point. However, 0 is an asymptotic value (the only one), and hence this point plays the same role as the critical points did for the previous two families. A point z is an *asymptotic value* if there is a curve $\gamma(t)$ which tends to the essential singularity as $t \to \infty$ but whose image tends to z as $t \to \infty$. Any curve whose real part tends to $-\infty$ has this property for E_λ.

Because E_λ has an essential singularity at ∞, the Julia set has one slightly different definition. In the previous cases, the Julia set was the boundary of the set of points whose orbits tend to ∞. Now the Julia set, $J(E_\lambda)$, is the **closure** of the set of points that escape to ∞. So any point whose orbit tends to ∞ is now in the Julia set.

When $\lambda > 0$, the dynamical behavior on the real axis is pretty simple. The graph of E_λ shows that there is a simple saddle-node bifurcation when $\lambda = 1/e$. See Figure 10. When $\lambda < 1/e$, there is an attracting fixed point a_λ and a repelling fixed point r_λ in $\mathbb{R}^+$. All points to the left of r_λ in $\mathbb{R}$ have orbits that tend to a_λ and hence do not lie in the Julia set, while the half-

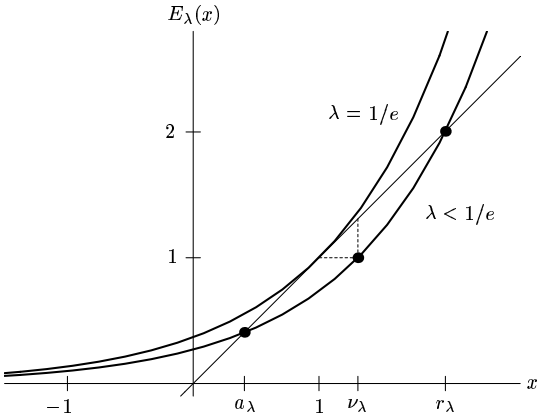

Figure 10: The graphs of E_λ for $\lambda = 1/e$ and $\lambda < 1/e$.

line $[r_\lambda, \infty)$ is in $J(E_\lambda)$. In fact, all points in $\mathbb{C}$ to the left of the vertical line through r_λ lie in the Fatou set. To see this, let x_λ be the point in $\mathbb{R}$ for which $E'_\lambda(x_\lambda) = 1$. So x_λ lies in the open interval (a_λ, r_λ). Then the vertical line through x_λ is mapped infinitely often around a circle centered at the origin which includes a_λ in its interior. Thus the open half-plane to the left of this vertical line is contracted inside the disk bounded by this circle. Hence, by the Contraction Mapping Principle, all points in this open half plane have orbits that tend to a_λ. Then one checks easily that all points to the left of the vertical line through r_λ eventually map inside this half-plane as well and so are also in the Fatou set.

When $\lambda = 1/e$, the two fixed points a_λ and r_λ merge and again all points to the left of this now neutral fixed point in $\mathbb{R}$ do not lie in the Julia set, while the fixed point and all points to the right of it in $\mathbb{R}$ again do lie in $J(E_\lambda)$. A similar argument as above then says that all points to the left of a vertical line through this fixed point in $\mathbb{C}$ also tend to the neutral fixed point and so are in the Fatou set.

When $\lambda > 1/e$, the fixed points in $\mathbb{R}$ disappear (they actually become complex), and now all points in $\mathbb{R}$ tend to ∞ under iteration and so lie in $J(E_\lambda)$. So it looks like the Julia set undergoes an abrupt change when λ increases through $1/e$. In fact, much more happens: a result of Goldberg and Keen [12] states that, if the orbit of the asymptotic value 0 tends to ∞,

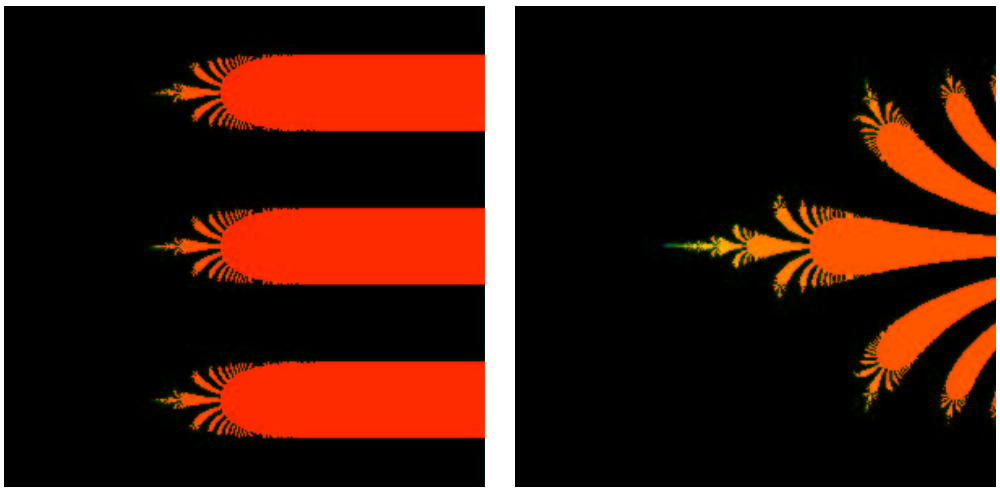

Figure 11: The Julia set for $E_{0.3}$ and a magnification along the real axis.

then the $J(E_\lambda)$ is the entire complex plane. So, for $\lambda \leq 1/e$, the Julia set is contained in the right half-plane, but, as soon as $\lambda > 1/e$, the Julia set becomes the entire complex plane.

Interestingly, no new periodic points are born as λ increases through $1/e$; all of the periodic points simply migrate continuously but do so in a way that they suddenly become dense in the plane when $\lambda > 1/e$. This is quite an interesting bifurcation!

In Figure 11, we display the Julia set for a value of $\lambda \in (0, 1/e)$. Black points are in the basin of attraction of a_λ and colored points escape to ∞. So the colored region is the Julia set. It appears that the Julia set contains open strips that tend off to ∞, but, By Montel's Theorem, this cannot happen. In fact, the Julia set in this case is a *Cantor bouquet*, a collection of uncountably many smooth curves which tend off to ∞ in the right half plane and each of which has a distinguished endpoint. See [7]. These curves are called "hairs" and all points (except the endpoints) have orbits that tend to ∞ and so are in the Julia set. For example, one hair is the subset of the real axis given by (r_λ, ∞); the endpoint is then the fixed point r_λ. Since the bounded orbits must lie in the set of endpoints, we have that the repelling periodic points must lie in the set of endpoints. Therefore this set is much more intricate than it at first seems: these endpoints must be everywhere dense in the Julia set. An interesting result of Mayer [14] shows that the only points that are

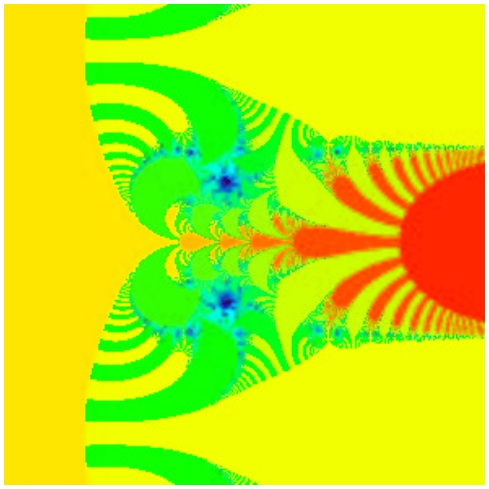

Figure 12: The Julia set for $E_{0.6}$ near the real axis.

accessible from the Fatou set are these endpoints; there is no curve contained in the Fatou set that limits on any single point in the hairs. Moreover, a result of Karpinska [13] shows that the Hausdorff dimension of the set of all points on the hairs is 1 whereas the Hausdorff dimension of the supposedly much smaller set of endpoints is 2!

In Figure 12 a portion of the Julia set for $\lambda = 0.6$ is displayed; here $J(E_{0.6}) = \mathbb{C}$. The two spirals actually converge down to the pair of repelling fixed points that appear after a_λ and r_λ coalesce and disappear off the real line.

As in the case of the other families discussed in this paper, we now turn briefly to the parameter plane for the complex exponential. In Figure 13 we display a portion of this parameter plane and a magnification near the origin. The cardioid shaped region is where E_λ has an attracting fixed point. The cusp of this cardioid is the parameter $\lambda = 1/e$. The large black region to the left of the cardioid actually extends to ∞ in the left half plane and contains parameters for which E_λ has an attracting cycle of period 2. Hanging off the cardioid are strips that all tend to ∞ in the right half-plane and contain parameters for which there is an attracting cycle of some period greater than 2. The two largest strips are regions where E_λ has an attracting cycle of period 3.

As in the case of the Julia sets, the colored regions contain parameters

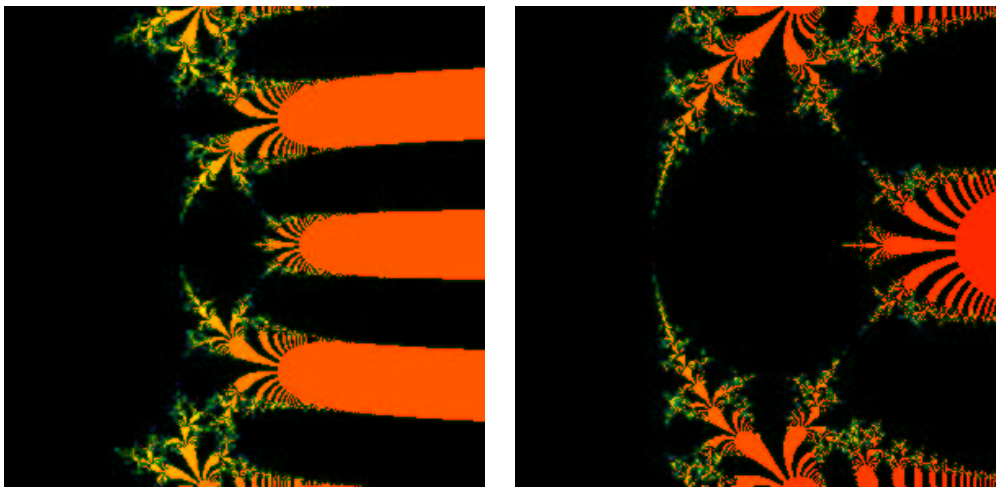

Figure 13: The parameter plane for E_λ.

for which the orbit of 0 tends to ∞ and so the Julia set for these parameters is the entire complex plane. Again as in the dynamical plane, these colored regions are really curves. For example, one such curve is the interval in $\mathbb{R}^+$ given by $(1/e, \infty)$.

References

[1] Buff, X. and Chéritat, A. The Yoccoz Function Continuously Estimates the Size of Siegel Disks. *Ann. Math.* **164** (2006), 265-312.

[2] Blanchard, P., Çilingir, F., Cuzzocreo, D., Devaney, R. L., Look, D. M., and Russell, E. D. Checkerboard Julia Sets for Rational Maps. *Int'l Journal of Bifurcation and Chaos* **23** (2013).

[3] Devaney, R. L. Singular Perturbations of Complex Polynomials. *Bull. Amer. Math. Soc.* **50** 2013.

[4] Devaney, R. L. The Mandelbrot Set, the Farey Tree, and the Fibonacci Sequence. *American Mathematical Monthly.* **106** (1999), 289-302.

[5] R. L. Devaney. The Fractal Geometry of the Mandelbrot Set: II. How to Add and How to Count. *Fractals* **3** No. 4, 1995, 629-640. See also `http://math.bu.edu/DYSYS/FRACGEOM2/FRACGEOM2.html`

[6] Devaney, R. L. Dynamics of $z^n + C/z^n$; Why the Case $n = 2$ is Crazy. In Conformal Dynamics and Hyperbolic Geometry. *Contemporary Math. AMS* **573** (2012), 49-65.

[7] Devaney, R. L. Complex Exponential Dynamics. In *Handbook of Dynamical Systems* **3**, Elsevier (2010), 125-224.

[8] Devaney, R. L. and Moreno Rocha, M. Geometry of the Antennas in the Mandelbrot Set. *Fractals.* **10** (2002), 39-46.

[9] Devaney, R. L., Look, D. M, and Uminsky, D. The Escape Trichotomy for Singularly Perturbed Rational Maps. *Indiana Univ. Math. J.* **54** (2005), 1621-1634.

[10] Devaney, R. L. and Pilgrim, K. M. Dynamic Classification of Escape Time Sierpinski Curve Julia Sets. *Fund. Math.* **202** (2009), 181-198.

[11] Douady, A. and Hubbard, J. Étude Dynamique des Polynômes Complexes. Partie I, *Publ. Math. D'Orsay* **84-02** (1984).

[12] Goldberg, L. and Keen, L. A Finiteness Theorem for a Dynamical Class of Entire Functions. *Ergodic Theory and Dynamical Systems.* **6** (1986), 183-192.

[13] Karpinska, B. On the Accessible Points in the Julia Sets for Entire Functions. *Fund. Math.* **180** (2003), 89-98.

[14] Mayer, J. An Explosion Point for the Set of Endpoints in the Julia Set of $\lambda \exp(z)$. *Ergodic Theory and Dynamical Systems.* **10** (1990), 177-184.

[15] McMullen, C. Automorphisms of Rational Maps. *Holomorphic Functions and Moduli*. Vol. 1. Math. Sci. Res. Inst. Publ. **10**. Springer, New York, 1988.

[16] Milnor, J. *Dynamics in One Complex Variable.* Princeton University Press (2006).

[17] Moreno Rocha, M. A Combinatorial Invariant for Escape Time Sierpinski Rational Maps. To appear.

[18] Qiu, W., Roesch, P., Wang, X., and Yin, Y. Hyperbolic Components of McMullen Maps. To appear.

[19] Shishikura, M. On the Quasiconformal Surgery of Rational Functions. *Ann. Sci. École Norm. Sup. Paris* **20**, 1-29.

[20] Whyburn, G. T. Topological Characterization of the Sierpinski Curve. *Fund. Math.* **45** (1958), 320-324.